



## ISTITUTO NAZIONALE DI RICERCA METROLOGICA Repository Istituzionale

### Modeling of Short-Term Synaptic Plasticity Effects in ZnO Nanowire-Based Memristors Using a Potentiation-Depression Rate Balance Equation

This is the author's accepted version of the contribution published as:

*Original*

Modeling of Short-Term Synaptic Plasticity Effects in ZnO Nanowire-Based Memristors Using a Potentiation-Depression Rate Balance Equation / Miranda, Enrique; Milano, Gianluca; Ricciardi, Carlo. - In: IEEE TRANSACTIONS ON NANOTECHNOLOGY. - ISSN 1536-125X. - 19:(2020), pp. 609-612. [10.1109/tnano.2020.3009734]

*Availability:*

This version is available at: 11696/64770 since: 2021-01-29T12:13:25Z

*Publisher:*

IEEE-INST ELECTRICAL ELECTRONICS ENGINEERS INC

*Published*

DOI:10.1109/tnano.2020.3009734

*Terms of use:*

This article is made available under terms and conditions as specified in the corresponding bibliographic description in the repository

*Publisher copyright*

IEEE

© 20XX IEEE. Personal use of this material is permitted. Permission from IEEE must be obtained for all other uses, in any current or future media, including reprinting/republishing this material for advertising or promotional purposes, creating new collective works, for resale or redistribution to servers or lists, or reuse of any copyrighted component of this work in other works

(Article begins on next page)

# Modeling of Short-Term Synaptic Plasticity Effects in ZnO Nanowire-Based Memristors Using a Potentiation-Depression Rate Balance Equation

E. Miranda, *Senior Member, IEEE*, G. Milano, C. Ricciardi

**Abstract**— This letter deals with short-term plasticity (STP) effects in the conduction characteristics of single crystalline ZnO nanowires, including potentiation, depression and relaxation phenomena. The electrical behavior of the structures is modeled following Chua's approach for memristive systems, *i.e.* one equation for the electron transport and one equation for the memory state of the device. Linear conduction is assumed in the first case together with a voltage-controlled rate balance equation for the normalized conductance. The devices are subject to electrical stimuli such as ramped and pulsed voltages of both polarities with varying amplitude and frequency. In either case, the proposed model is able to account for the STP effects exhibited by ZnO highlighting its neuromorphic capabilities for bio-inspired circuits. An equivalent circuit representation and the SPICE implementation of the complete model is also provided.

**Index Terms**—ZnO, nanowire, short-term plasticity, memristor

## I. INTRODUCTION

SINGLE isolated nanowires (NWs) represent suitable model systems to investigate nanoionic properties underlying resistive switching (RS) phenomena in unconventional memristive structures [1]. In particular, zinc oxide (ZnO)-NW has attracted wide attention because of its remarkable functionalities as an artificial synapse [2,3] exhibiting clear signs of short-term plasticity (STP) effects [4]. Ag and Pt are investigated here as representatives of electroactive and inert electrode materials, respectively. One distinctive feature of the ZnO-NW RS behavior is that the metal ion ( $\text{Ag}^+$ ) migration responsible for the change of conduction state takes place exclusively on the crystal surface [3], different from the vast majority of memristive devices in which internal filamentary switching is the leading mechanism [5]. In order to model STP effects in ZnO-NW including potentiation (current increase), depression and relaxation (current decrease) caused by external electrical stimulation, a memristive model comprising one equation for the electron transport and one equation for the ion displacement is proposed. Electron flow through the structure is modeled by conductance modulation of the ionic pathway driven by a voltage-dependent rate balance equation. Since this is an electrical model in the realm of Chua's approach [6], no attempt is made here to connect the proposed

equations with the microscopic physics although the forward and backward ionic diffusive processes are somehow represented by their respective rate coefficients. Besides reporting the analytic solution to the hysteretic conduction problem using a spreadsheet implementable recursive method, an equivalent electrical circuit for the whole memristive model is provided. A compact model of this kind for the elementary structure is of utmost importance for simulating large NW networks driven by arbitrary input signals [1].

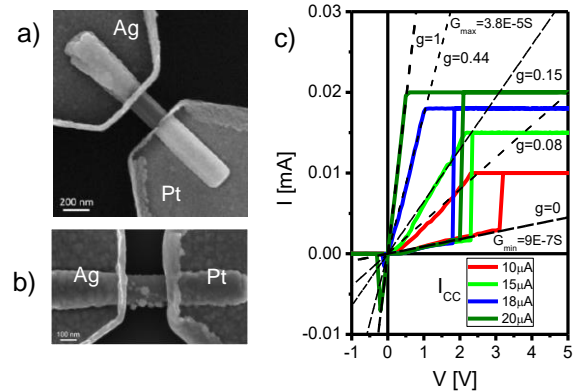


Fig. 1: a) SEM image of an Ag/ZnO-NW/Pt structure. b) Image of the structure after electroforming showing the formation of an Ag conducting path on the NW surface. c) Typical bipolar RS  $I$ - $V$  characteristics after electroforming using different current compliances ( $I_{cc}$ ).  $g$  is the normalized conductance.

## II. DEVICES AND EXPERIMENTAL SETUP

Single crystal ZnO-NW-based memristive devices (Fig.1.a) were fabricated by combining optical and e-beam lithography (EBL) [1,3]. Optical lithography was used to pattern sub-millimetric probe circuits using a customized mask on a  $\text{SiO}_2$ (450 nm)/p-Si substrate. Pads and probe paths geometries were realized by sputtering deposition of Ti/Au followed by a lift-off process in acetone. NWs were mechanically transferred from the growth substrate to a  $\sim 120 \times 120 \mu\text{m}^2$  selected area of the probe circuit using a mounted hair and an optical microscope. The NW location on the substrate was referenced by using proper markers and SEM imaging. Devices were treated with oxygen plasma before the metal (Ag and Pt) deposition. Figure 1.b reveals the presence of an Ag conducting path after the electroforming step (not shown here). DC

electrical characterization was carried out with a Keithley 2636A and a Keithley 4200 semiconductor parameter analyzer. Figure 1.c shows the effect of different current compliances ( $I_{cc}$ ) on the bipolar switching curves. Notice the large asymmetry between the set (2-3 V) and reset voltages ( $\approx -0.25$ -0.5 V).

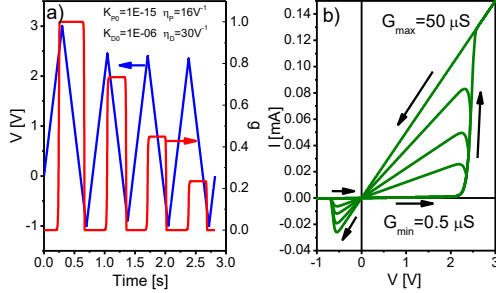


Fig. 2: a) Positive and negative voltage ramps and evolution of the device memory state as a function of time. b) Set and reset  $I$ - $V$  loops generated by the input signal shown in a).

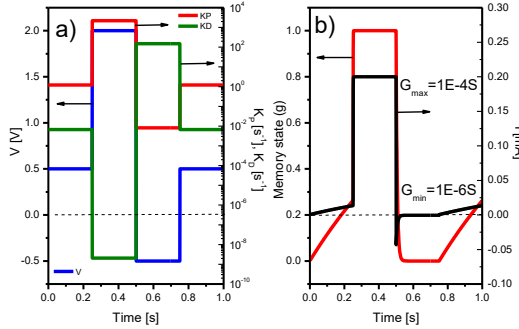


Fig. 3: a) Evolution of the P-D coefficients as a function of voltage and time. b) Evolution of the memory state and current for the input signal shown in a). Notice how the negative voltage pulse erases the memory state of the device.

### III. MEMRISTIVE MODEL FOR ZNO NANOWIRES

According to the experimental results shown in Fig.1.c, intermediate conduction states in the Ag/ZnO-NW/Pt structure after electroforming can be approximately described by the linear relationship [7]:

$$I = [G_{MIN}(1 - g) + G_{MAX}g]V \quad (1)$$

where  $0 \leq g \leq 1$  is the normalized conductance.  $G_{MAX}$  and  $G_{MIN}$  are the maximum and minimum experimental conductances, respectively, used for model calibration. The state equation for the synaptic properties of the NW is expressed as:

$$\frac{dg}{dt} = \kappa_P(V)(1 - g) - \kappa_D(V)g \quad (2)$$

where  $\kappa_P$  and  $\kappa_D$  are the potentiation and depression (P-D) rate coefficients, respectively. (2) is a rate balance equation [8] which accounts for the transmission properties of the ions contributing to the system conductance. For the sake of simplicity, here,  $\kappa_P$  and  $\kappa_D$  are assumed to be functions of the applied voltage  $V$  exclusively:

$$\kappa_{P,D}(V) = \kappa_{P0,D0} \exp(\pm \eta_{P,D} V) \quad (3)$$

as expected for a diffusive ionic process [9-11].  $\kappa_{P0,D0} > 0$  are fitting constants and  $\eta_{P,D} > 0$  are transitions rates. Notice that, more in general, depending on the functional dependence of  $\kappa_P$

and  $\kappa_D$  on  $V$ , (2) can cover a wide variety of situations including induced ( $\eta_D(V > 0) > 0$ ) or spontaneous ( $\eta_D(V > 0) = 0$ ) relaxation.

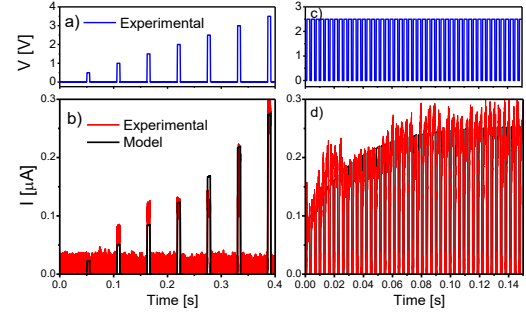


Fig. 4: a) and b) Effect of isolated increasing voltage pulses on the  $I$ - $t$  curve. c) and d) Effect of paired pulse facilitation (PPF) on the  $I$ - $t$  curve.

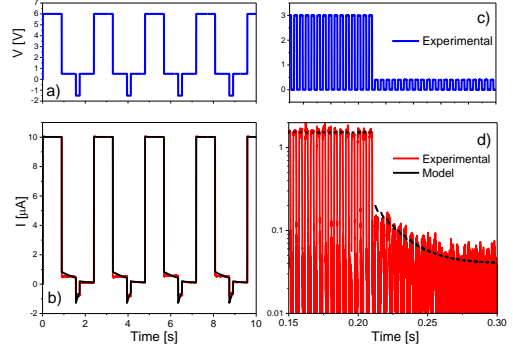


Fig. 5: a) and b) Effect of positive and negative pulses on the  $I$ - $t$  curve. c) and d) Effect of abrupt voltage reduction with current transient.

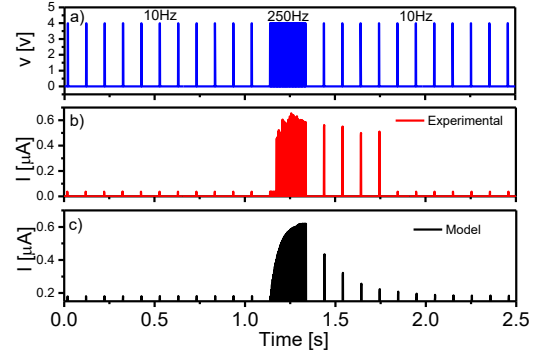


Fig. 6: a) Sequence of voltage pulses with a frequency change. b) and c) Experimental and model curves showing the accumulation effect.

Assuming a simulation timestep  $\Delta t > 0$ , (2) can be recursively solved as:

$$g_t = \frac{\kappa_P}{\kappa_P + \kappa_D} \left\{ 1 - \left[ 1 - \left( 1 + \frac{\kappa_D}{\kappa_P} \right) g_{t-1} \right] e^{-(\kappa_P + \kappa_D) \Delta t} \right\} \quad (4)$$

where  $g_t$  and  $g_{t-1}$  are the normalized conductances at times  $t$  and  $t-1$ , respectively.  $g_0$  is the initial value  $g(t=0)$ . Notice that solution (4) is not expressed in the standard way as a continuous function of  $t$  because of the hysteretic nature of the problem we are dealing with. (4) allows us to simulate cases in which the input voltage is arbitrary including pulsed measurements. While Fig. 2 illustrates the effects of positive and negative voltage ramps on the state variable (Fig. 2a) and the corresponding current loops generated by (1) and (2) (Fig. 2b), Fig. 3 shows P-D coefficient variations (Fig. 3a) and their effects on the  $g$ - $t$  and  $I$ - $t$  curves (Fig. 3b), respectively. Notice

that, depending on the bias polarity,  $\kappa_P$  and  $\kappa_D$  can differ in several orders of magnitude. Figures 2 and 3 are only aimed at emphasizing the writing/erasing behavioral aspect of the model and do not correspond to real experiments.

#### IV. MODEL AND EXPERIMENTAL RESULTS

In order to test the ability of the proposed model to account for the neuromorphic capabilities of ZnO-NWs, devices were subject to a variety of electrical stimuli and simulated first using expression (4). Figures 4.a and 4.b illustrate the effects of isolated voltage pulses of increasing amplitude on the current magnitude. However, the combined time-voltage action can be seen in Figs. 4.c and 4.d, which show the accumulated effect of a train of pulses of equal magnitude (2.5 V) emulating paired-pulse facilitation (PPF) [12]. Notice that large fluctuations and variability, as expected for an ionic filamentary path, are observed. Figure 5.a shows the case of a sequence of large positive pulses (6 V) with intermediate reset pulses (-1.5 V). As illustrated in Fig. 5.b, the negative pulses partially wipe out the memory of the device so that the currents measured at 0.5 V before and after the pulses are dissimilar. This is the depression mechanism operating at negative voltages (reset process). However, as shown in Figs. 5.c and 5.d, it is also possible to detect in some cases long transient effects on the current behavior after reducing the input signal [13]. This is the result of depression associated with the relaxation mechanism operating at positive voltages (also called forgetting effect related to STP [10,14]). The occurrence of this effect is supported by the experiment illustrated in Fig.6, in which, first, a sequence of constant voltage (4 V) low frequency (10 Hz) spikes is applied to the device. Under this circumstance, the current keeps low. However, when the spiking frequency increases to 250 Hz at approximately 1.2 s, the current rises because of the PPF effect. After reducing the spiking frequency to the initial value, the current decays back to the previous level. Remarkably, relaxation takes place without changing the bias polarity and magnitude of the spikes. This is a natural consequence of the short-term memory effect of the device.

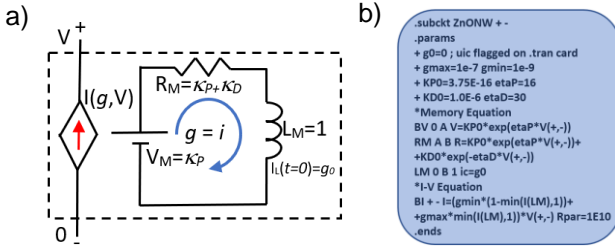


Fig. 7: a) Schematic of the equivalent circuit model for Eqns. (1) and (2). + and - are the device terminals. The RL circuit represents the device memory. b) LTSpice script for the equivalent circuit in a).  $0 \leq g_0 \leq 1$  is the initial memory state.

#### V. EQUIVALENT CIRCUIT MODEL

Although (4) is the analytic solution to (2) and can be used for arbitrary input signals, it requires considering a predefined

simulation timestep  $\Delta t$ . On the other hand, (2) can be represented by a series RL circuit with  $V$ -dependent parameters. The differential equation for the RL circuit shown in Fig. 7a reads:

$$L_M \frac{di}{dt} + R_M i = V_M \quad (5)$$

so that if we take  $i=g$  and  $L_M=1$  in (5), then from (2),  $R_M=\kappa_P + \kappa_D$  and  $V_M=\kappa_P$ . The complete model schematic (two-port  $I$ - $V$  and memory circuit) for the ZnO NW-electrodes system and its LTSpice [15] implementation are shown in Figs. 7a and 7b, respectively. + and - indicate the terminals of the NW. Alternative expressions for the P-D coefficients, more complex or realistic than those specified by (3), can be investigated as well by editing the subcircuit code provided in Fig.7.b. Interestingly, (5) expresses the connection between the memory effect of memristors and its associated inductive behavior [16].

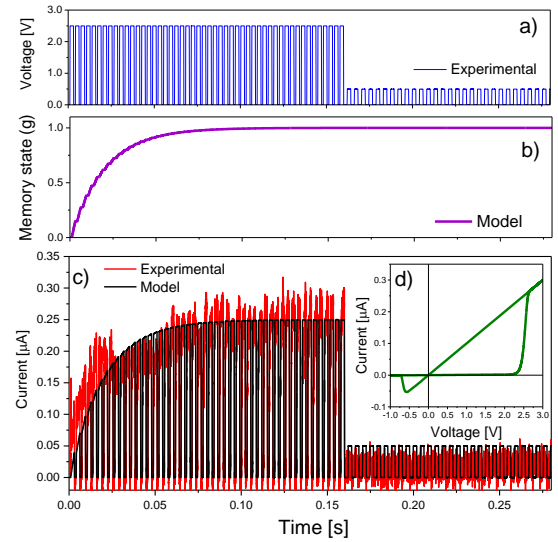


Fig. 8: a) Experimental voltage sequence. b) Evolution of the memory state of the device as a function of time. c) Experimental (red line) and model (black line)  $I$ - $t$  characteristic. d) Simulated  $I$ - $V$  curve. Model script and parameters used for simulation in LTSpice are shown in Fig. 7b.

As a first application example of the equivalent circuit representation, Fig. 8 illustrates experimental and model results corresponding to the potentiation effect of the memory state followed by a sudden reduction of the bias condition. The circuit depicted in Fig. 7a is fed using the experimental voltage sequence shown in Fig. 8a. Model script and parameters used to simulate the curves are those shown in Fig. 7b. As shown in Fig. 8b, the memory state increases until saturation. The simulated  $I$ - $t$  curve is presented in Fig. 8c. Relaxation effects, as those seen in Figs. 5d and 6b, are not detected here. Observation of a second potentiation would require the action of the depression mechanism at positive bias. Additionally, Fig. 8d shows the corresponding  $I$ - $V$  characteristic. The loop exhibits the high and low resistance states as well as the high asymmetry between the set and reset voltages typical of the ZnO-NW system ( $V_{SET} \approx -\ln(\kappa_{P0})/\eta_P$ ,  $V_{RESET} \approx \ln(\kappa_{D0})/\eta_D$ ).

As a second case study, we show the ability of the proposed approach to simulate more complex behaviors. In this case, two



opposite-biased identical memristors (same parameters as in the previous example but  $g_{01}=0$  and  $g_{02}=1$ ) forming a complementary resistive switching (CRS) device. This is a simple though emblematic network to demonstrate the model connectivity capacity [17]. In this particular case, the large asymmetry between set and reset voltages plays a central role in the overall curve behavior. A sinusoidal input signal with 3V amplitude and 1Hz frequency was considered for this simulation exercise. Notice the peaks in the red line  $I$ - $V$  (Fig. 9a) and  $I$ - $t$  (Fig. 9b) curves associated with the simultaneous activation of both devices. The circuit is illustrated in Fig. 9a's inset. Simulations of this kind allows determining how the applied potential drops in each device. The extension to larger ZnO-NW networks is straightforward.

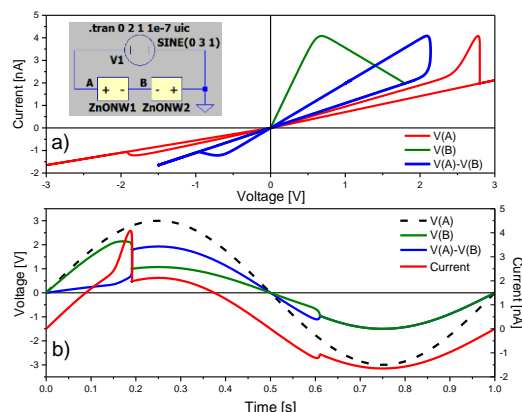


Fig. 9. a)  $I$ - $V$  characteristics corresponding to the different potential drops occurring across each device in a CRS configuration. The circuit scheme is shown in the inset. b) Corresponding  $I$ - $t$  and  $V$ - $t$  curves.

## VI. CONCLUSIONS

In this letter, short-term synaptic plasticity effects in the conduction characteristic of single crystalline ZnO-NWs attached to Ag and Pt metal electrodes were investigated. The devices were subject to a variety of electrical stimuli including voltage ramps and pulses. To account for STP phenomena including potentiation, depression and relaxation, a simple memristive model that considers the coupled action of electron and ionic transport represented by linear conduction and a rate balance equation, respectively, was proposed. It was also shown how the reported model admits a compact circuital description. As demonstrated, ZnO-NW exhibits remarkable features for bio-inspired circuit applications which can be realistically simulated using memristor theory in the context of a circuit simulator.

## REFERENCES

- [1] G. Milano, S. Porro, I. Valov, C. Ricciardi, "Recent developments and perspective for memristive devices based on metal oxide nanowires," *Adv Electron Mater*, vol. 9, 1800909, March, 2019. DOI: 10.1002/aelm.201800909
- [2] M. Laurenti, S. Porro, C. Pirri, C. Ricciardi, A. Chiolerio, "Zinc oxide thin films for memristive devices: a review," *Crit Rev Solid St Mat Sci*, vol. 42, pp.153-172, 2017. DOI: 10.1080/10408436.2016.1192988

- [3] G. Milano, M. Luebben, Z. Ma, R. Dunin-Borkowski, L. Boarino, C. Pirri, R. Waser, C. Ricciardi, I. Valov, "Self-limited single nanowire systems combining all-in-one memristive and neuromorphic functionalities," *Nat Comm*, vol. 9, 5151, December, 2018. DOI: 10.1038/s41467-018-07330-7
- [4] S. Wu, K. Michael Wong, M. Tsodyks, Eds., *Neural information processing with dynamical synapses*, Frontiers E-books, Frontiers in Computational Neuroscience, vol. 7, 2013. DOI: 10.3389/978-2-88919-383-7
- [5] C. Sung, H. Hwang, I. Yoo, "Perspective: A review on memristive hardware for neuromorphic computation," *J Appl Phys*, vol. 124, 151903, October, 2018. DOI: 10.1063/1.5037835
- [6] L. Chua, "Resistance switching memories are memristors," *Appl Phys A*, vol. 102, pp.765-783, March, 2011. DOI: 10.1007/s00339-011-6264-9
- [7] D. Strukov, G. Snider, D. Stewart, R.S Williams, "The missing memristor found," *Nature*, vol. 453, pp.80-83, March, 2008. DOI: 10.1038/nature06932
- [8] J. Carroll, *Rate equations in semiconductor electronics*, Cambridge University Press, Cambridge, 1986. DOI: 10.1017/CBO9780511622489
- [9] S. Menzel, S. Tappertzhofen, R. Waser, I. Valov, "Switching kinetics of electrochemical metallization memory cells," *Phys Chem Phys*, vol. 15, pp.6945-6952, March, 2013. DOI: 10.1039/c3cp50738f
- [10] Z. Wang, A. Joshi, S. Savelev, H. Jiang, R. Midya, P. Lin, M. Hu, N. Ge, J. Strachan, Z. Li, Q. Wu, M. Barnell, G. Li, H. Xin, R. Stanley Williams, Q. Xia, J Yang, "Memristors with diffusive dynamics as synaptic emulators for neuromorphic computing," *Nat Mat*, vol. 16, pp.101-108, September, 2017. DOI: 10.1038/nmat4756
- [11] A. Rodriguez-Fernandez, C. Cagli, J. Suñé, E. Miranda, "Switching voltage and time statistics of filamentary conductive paths in HfO<sub>2</sub>-based ReRAM devices," *IEEE Electron Dev Lett*, vol. 39, pp.656-659, May, 2018. DOI: 10.1109/LED.2018.2822047
- [12] S. Deswa, A. Kumar, A. Kumar, "NbOx based memristor as astrifical synapse emulating short term plasticity," *AIP Advances* 9, 095022 (2019). DOI: 10.1063/1.5118980.
- [13] S. Lee, J. Park, M. Lee, J. Bolland, "Multilevel resistance in ZnO nanowires memristors enabled by hydrogen annealing treatment," *AIP Adv*, vol. 6, 125010, December, 2016. DOI: 10.1063/1.4971820
- [14] E. Zhou, L. Fang, B. Yang, "A general method to describe forgetting effect of memristors," *Phys Lett A*, vol. 383, pp.942-948, March, 2019. DOI: 10.1016/j.physleta.2018.12.028
- [15] G. Brocard, "The LTspice IV simulator: manual, methods and applications," *Wurth Elektronik*, 2013. ISBN 978-3899292589
- [16] S. Dueñas, H. Castán, H. García, O. Ossorio, L. Domínguez, E. Miranda, "Experimental observation of negative susceptance in HfO<sub>2</sub>-based RRAM devices," *IEEE Electron Dev Lett*, vol. 38, pp.1216-1219, September, 2017. DOI: 10.1109/LED.2017.2723054
- [17] E. Linn, A. Siemon, R. Waser, S. Menzel, "Applicability of well-established memristive models for simulations of resistive switching devices," *IEEE Trans Circ Syst I*, vol. 61, pp. 2402-2410, July, 2014. DOI: 10.1109/TCSI.2014.2332261